Journal of
Synchrotron
Radiation

ISSN 1600-5775

Received 3 September 2013
Accepted 23 February 2014

Synchrotron far-infrared spectroscopy of corroded steel surfaces using a variable angle of incidence

Kateřina Lepková,* Wilhelm van Bronswijk, Vedapriya Pandarinathan and Rolf Gubner

Corrosion Centre for Education, Research and Technology, Department of Chemistry, Curtin University, GPO Box U1987, Perth, WA 6845, Australia. *E-mail: k.lepkova@curtin.edu.au

Far-infrared spectroscopy, using a synchrotron source, has been used to study carbon steel corroded in CO_2-saturated brine in the presence and absence of the corrosion inhibitor 2-mercaptopyrimidine (MPY), which allowed the steel surface roughness to be modified. The effect of the angle of incidence (θ_i, 30–80°) on the band intensity and observed bands of the spectra from these surfaces has been determined. For the MPY-treated steel (low surface roughness) the highest band intensity is observed at high θ_i (80°) and different bands were observed at different θ_i. In contrast, for the MPY-free steel (high surface roughness) the highest band intensity is observed at low θ_i (30°) and spectral content changes were not observed. The results are explained in terms of the roughness of the MPY-treated and MPY-free steels, and their effect on the level of diffusely reflected light of the incident infrared beam.

Keywords: far-infrared spectroscopy; incidence angle; absorption intensity; surface roughness; corrosion; corrosion inhibitor.

1. Introduction

Examination of thin films at corroded metallic surfaces by far-infrared (FIR) spectroscopy is generally limited by low absorption intensity in the spectra. The low absorption intensity can be improved by application of synchrotron-sourced infrared radiation that provides an infrared beam of greater brightness in comparison with conventional infrared sources and thus increases the signal-to-noise ratio of the absorption bands in the spectra. Synchrotron-sourced FIR spectroscopy has been applied in studies of thin films at metallic substrates such as copper and gold (Melendres *et al.*, 1998, 2000; Melendres & Hahn, 1999; Hahn & Melendres, 2010). Of these studies, few have used accessories that utilize a selectable angle of incidence at which the infrared beam approaches the surface (Hahn *et al.*, 2007, 2008). It has been shown that the increase of the incidence angle can enhance the absorption intensity at microscopically smooth surfaces with the best result achieved using a polarized beam at high angles of incidence close to the grazing angle (Francis & Ellison, 1959; Greenler, 1966). At rough surfaces, the relationship between the incidence angle and the absorption intensity becomes more complex because the intensity is also affected by the roughness of the surface. This is due to the combination of specular and diffuse reflectance of the infrared beam that is distributed into various directions from its original specular path. When the original beam is diffusely reflected, less signal reaches the detector which can result in low absorption intensity in the spectra.

The present study introduces the application of FIR with a variable incidence angle to the analysis of corrosion-roughened surfaces. The aim is to determine the effect of the incidence angle on the absorption intensity and the spectral content with respect to the roughness of the studied surface, and thereby define the optimal measurement parameters for FIR analysis at topographically uneven surfaces.

Surfaces of variable roughness were prepared by exposing carbon steel samples to CO_2-saturated brine in the presence or absence of a corrosion inhibitor, 2-mercaptopyrimidine (MPY). Steel surfaces exposed to CO_2-saturated brine (without a corrosion inhibitor) are generally roughened by dissolution of the metallic substrate and/or by deposition of a surface film while MPY forms stable complexes at the steel surface (Reznik *et al.*, 2008) and thus hinders the corrosion reactions that would otherwise increase the surface roughness. These two corroded steels with low (MPY-treated) and high (MPY-free) surface roughness are examined here by FIR at incidence angles of 30, 55 and 80° in order to investigate whether the absorption intensity can be optimized by varying the incidence angle. This is related to the specular and diffusion reflectance of the infrared beam from the topographically uneven surfaces. The two surfaces selected for this study closely resemble real industrial systems.

2. Experimental

2.1. Materials and methods

The carbon steel studied had the following elemental composition (wt%): C 0.37, Mn 0.80, Si 0.28, Cr 0.09, P 0.01, Ni 0.01, Fe balance. Steel samples (25 mm × 52 mm) were polished to 1200 grit, cleaned with methanol and ultra-pure deionized water and dried with nitrogen prior to immersion in the test solution at 353 K for 24 h. The samples were rinsed with ultra-pure deionized water and dried with nitrogen after the immersion and stored under vacuum until further analysis. Care was taken when handling the samples to minimize their exposure to air.

The testing solutions were: (1) brine, consisting of 0.5 M sodium chloride (NaCl; Ajax Finechem, 99.9%) and 1×10^{-3} M sodium hydrogen carbonate ($NaHCO_3$; Merck, 99.5%), and (2) brine with 500 ppm of 2-mercaptopyrimidine ($C_4H_4N_2S$; Sigma-Aldrich, 98%). Solutions (1) and (2) were used to prepare samples with high and low surface roughness, respectively. Testing solutions were saturated with high-purity carbon dioxide (99.99%) before and during the experiments. The molecular structure of the corrosion inhibitor MPY is shown in Fig. 1.

2.2. Surface roughness measurements

The roughness of the steel surfaces was measured using an Alicona Infinite Focus visible-light microscope (Alicona Imaging GmbH, Austria). The samples were briefly exposed to air during the surface roughness measurements.

A surface roughness parameter R_q (root mean square) was calculated from the surface heights using the Alicona IFM 3.5 software. The roughness measurements were carried out over a total surface area of 6 mm^2 and performed in a detailed scale (steps of 0.07 mm^2) using a 50× magnification objective at the microscope. Analysing this large surface area in the high-resolution small steps assured accurate examination of the surface with local surface irregularities taken into account.

2.3. Synchrotron infrared spectral measurements and analysis

The infrared spectroscopy analysis was performed at the Far-infrared and high-resolution beamline of the Australian Synchrotron, using a Brüker IFS 125/HR Fourier transform spectrometer with a variable incidence angle (VIA) reflectance accessory (VeeMAX, PIKE Technologies). A Si bolometer detector, mylar multilayer beamsplitter and 4 mm aperture were used. The FIR single-channel spectra were recorded in absorbance mode at a resolution of 2 cm^{-1} over the range 700–30 cm^{-1} with 200 scans being averaged. Each spectrum presented in this work was calculated as $-\log(I/I_0)$, where I and I_0 represent the intensity of the single-channel (single-beam) spectra collected from the sample and background (gold mirror), respectively. The spectral analysis was performed using Opus 6.5 software (Brüker Optics).

The samples were positioned in a holder in the VIA accessory with the exact position of the sample in the holder marked to ensure that the same surface area was re-examined at different incidence angles (30, 55 and 80° with respect to the surface normal). The accessory was placed into an enclosed nitrogen-purged compartment in the FIR spectrometer, evacuated and samples kept under vacuum before, during and after the analysis.

2.3.1. Optical parameters. The FIR beamline at the Australian Synchrotron uses edge radiation which is radially polarized. The polarization vector rotates resulting in a p:s polarization distribution of 1:1 (50%:50%) near the grazing angle and predominant s polarization at the surface normal. A polarizer was not used in conjunction with this work as maximum brightness was deemed to be advantageous and its introduction to the beam path could significantly reduce the radiation reaching the detector. Also, the roughness of corroded surfaces and formation of corrosion products would in all likelihood preclude obtaining orientation information for adsorbed species and hence s and p polarization studies were not pursued. Depending on the extent of corrosion and roughness of the surface, the spectra will have contributions from both specular and diffuse reflectance of corrosion products as well as reflectance/absorbance of surface-adsorbed species. It is to be expected that for non-homogeneous corroded surfaces with high roughness both the specular and diffuse reflectance will take place, with diffuse reflectance being the predominant component of the reflected beam. At homogeneous surfaces with low surface roughness, maximum absorption intensity is expected at high incidence angles (close to grazing angle) due to increased contribution of the p-polarization vector in the incidence beam.

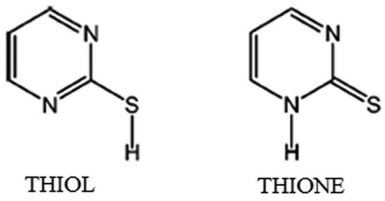

Figure 1
Chemical structure of 2-mercaptopyrimidine thiol and thione tautomers.

3. Results and discussion

Figs. 2 and 3 show infrared spectra recorded at variable incidence angles at steels treated with and without the MPY present in the CO_2-saturated brine, respectively. No absorption bands other than those presented were found in the wavenumber region 700–30 cm^{-1}.

The results from the MPY-treated steel (Fig. 2) show that the highest absorption intensity is obtained at an incidence angle of 80° in the 350–200 cm^{-1} range. Increasing the incidence angle from 30° to 80° results in increases in the absorption intensity, and a change in relative intensities of the absorption bands, particularly around 300–200 cm^{-1}. These changes are attributed to the increased p-polarization vector of the incident radiation with increasing angle of incidence and hence the intensity increases of the absorption bands. The

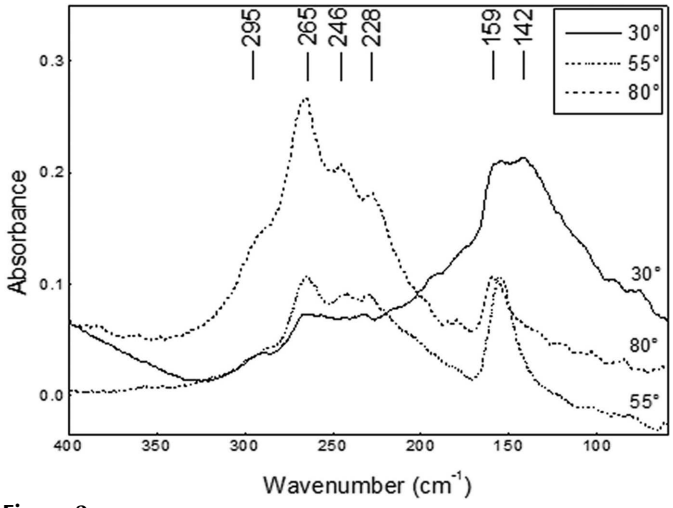

Figure 2
Far-infrared reflectance spectra recorded at variable angles of incidence from carbon steel treated in CO_2-saturated brine in the presence of corrosion inhibitor MPY.

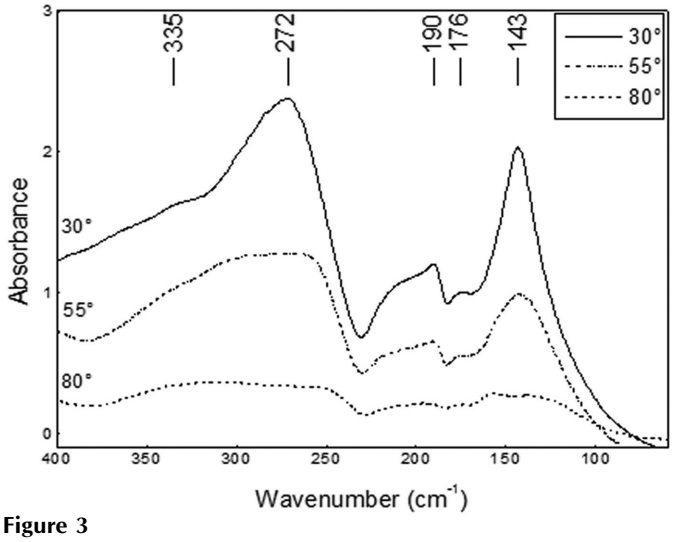

Figure 3
Far-infrared reflectance spectra recorded at variable angles of incidence from carbon steel treated in CO_2-saturated brine in the absence of corrosion inhibitor MPY.

absorption intensity of the band near 159 cm^{-1} appears to be less dependent on the angle of incidence, and the spectrum recorded at 30° reveals an additional absorption band at 142 cm^{-1} which was not seen at the higher incidence angles. These differences can be related to the variations in path-length and area coverage of the infrared beam with different incidence angles and possibly the form of the adsorbed MPY molecule, which is discussed later.

For the MPY-free steel (Fig. 3), the high absorption intensities are due to the diffuse reflectance loss, which was indicated by intensity differences in the single-channel spectra from the steel and the gold mirror. The spectrum with the highest absorption intensities is obtained at the incidence angle of 30°. The absorption intensity decreases with increasing incidence angle and again some change in relative intensities is observed. The decrease in intensity with increasing incidence angle can be explained in terms of diffuse reflectance and the VIA geometry.

3.1. Effect of incidence angle with respect to surface roughness

The results in Figs. 2 and 3 confirm the fundamental point of this work that the incidence angle can affect the spectral content (absorption bands) observed, affects the absorption intensity and that a wider range of information can be achieved by analysis utilizing a range of incidence angles. This is best seen in the spectra recorded using incidence angles of 80° and 30° at the MPY-treated and the MPY-free surfaces, respectively. It is clear that the positions of all the absorption bands observable in these spectra could not be determined from spectra recorded at a single incidence angle.

Comparison of the spectra in Figs. 2 and 3 show that the relationship between the absorption intensity and the angle of incidence follows the opposite trend for the two studied surfaces: at the MPY-treated surface (region above 200 cm^{-1}) the absorption intensity increases with increasing angle of incidence, whereas at the MPY-free surface the absorption intensity decreases with increasing angle of incidence. The effect of incidence angle on the absorption intensity of the MPY-treated and MPY-free steels is attributed to the difference in their surface roughness. The MPY-treated and MPY-free steels have a surface roughness parameter R_q of 0.58 μm and 4.33 μm, respectively. For comparison, R_q obtained from non-corroded steel is 0.37 μm.

The surface selection rule applies for steels with low surface roughness and in the absence of significant diffusion reflectance. The polarization of the incidence beam in this work is 50% *s* and 50% *p* near the grazing angle and changes to *s*-polarization at angles near normal (see also §2.3.1). This is supported by high absorption intensity in the infrared spectra shown in Fig. 2, where low-roughness surface steel (MPY-treated) gives a good intensity at all angles and the highest absorption intensity at 80° (region above 200 cm^{-1}). It should be noted, however, that a small amount of diffusion reflectance is still likely to occur at the MPY-treated steel (R_q = 0.58 μm). The intensity of the diffusely reflected beam can be measured from surfaces with roughness as low as R_q = 0.2 μm (Li Voti *et al.*, 2009). However, the amount of diffuse reflectance loss from the MPY-treated surface is considered insignificant for the purpose of this study as the results presented here follow the rules of specular reflection typical for microscopically smooth surfaces. The results demonstrate that high incidence angles are suitable for the FIR analysis of carbon steels with low surface roughness.

Besides the obvious advantage of the grazing angle in the analysis of thin surface films at the surfaces with low roughness, the results in Fig. 2 also show that additional spectral features may be observed at low angles of incidence. The spectra recorded at incidence angle of 30° revealed an additional absorption band at 142 cm^{-1}, which was not observed at higher incidence angles (55° and 80°). This indicates that using a range of angles of incidence at low-roughness corroded

surfaces can be useful for a complete analysis of those surfaces.

At the MPY-free steel with high surface roughness and if corrosion products are present, the uneven surface topography results in diversion of the infrared beam from its original path and the produced spectra can be characterized as DRIFT spectra. At high angles of incidence, the effect of irregular reflection planes and corrosion products that cause diffuse reflectance and scatter of the infrared beam is decreased. The results in Fig. 3 show that the highest absorption intensity at highly rough surfaces is achieved by the use of low angles of incidence that are close to the surface normal and that the spectral content does not change dramatically with angle of incidence. The latter is to be expected as the spectra would derive from diffuse and specular reflectance by the corrosion products. At 30° there would be maximum penetration of the pits and crevices in the surface leading to a maximum DRIFT signal. As the angle of incidence increases, there is less penetration of these pits and crevices and more specular reflectance from unpitted parts of the surface, leading to the observed response.

In most cases the degree of surface roughness is unknown prior to the infrared analysis and the ideal incidence angle cannot be pre-selected. The results presented here demonstrate that by using a wide range of incidence angles the absorption intensity and the spectral information can be improved for surfaces with low roughness and surfaces with high roughness.

3.2. Assignment of absorption bands

Definitive assignment of the absorption bands would require a detailed FIR analysis of the range of corrosion products formed on steels corroded under CO_2 conditions. Such analysis is beyond the scope of this work and will be the subject of a further investigation. However, tentative assignment of the absorption bands can be made based on comparison with literature data.

Fig. 4 shows the FIR spectrum of pure MPY powder. The absorption bands in the region below 200 cm^{-1} can be assigned to the aromatic ring torsions. Similarly, the band at 317 cm^{-1} is due to C—H out-of-plane distortion or to S—H torsion (Tripathi & Clements, 2003; Nowak *et al.*, 1991). Previous adsorption studies have shown that the appearance of these bands depends on the molecular (tautomeric) form of MPY, with thiol ($C_4H_3N_2SH$) at 143 cm^{-1} and thione ($C_4H_3N_2(H)S$) at 152 cm^{-1} (Tripathi & Clements, 2003). MPY is an almost planar molecule with only the H—(S) being out of plane (Fig. 1). Hence, only out-of-plane deformations of these molecules are going to produce spectra if it adsorbs in a planar or near-planar mode. MPY has been shown to adsorb in both planar and vertical orientation at silver surfaces depending on the presence and absence of Cl^- ions in the solution, respectively (Tripathi & Clements, 2003). A similar effect of chloride ions on an inhibitor adsorption has been shown for iron surfaces (Aramaki *et al.*, 1992), which is relevant to this work where the chloride-containing solution (brine) is used.

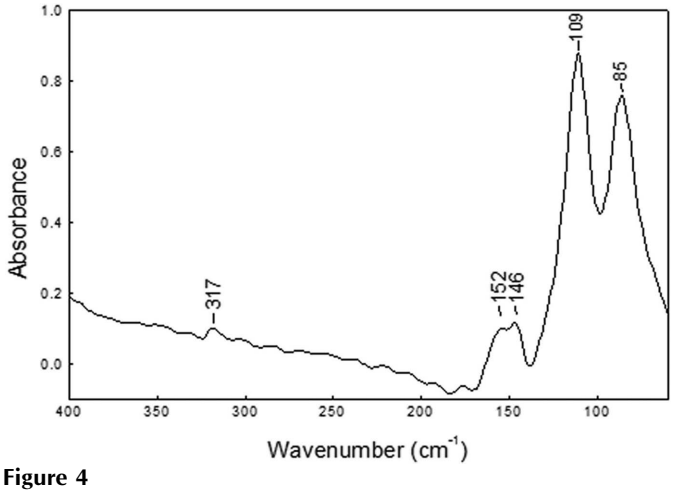

Figure 4
Far-infrared reflectance spectrum of pure MPY powder.

For the MPY-treated steel (Fig. 2), the positions of the major absorption bands are 159, 228, 246 and 265 cm^{-1}, with a shoulder band at 295 cm^{-1} from the spectrum recorded at an incidence angle of 80°. An additional absorption band was observed at 142 cm^{-1} at an incidence angle of 30°.

The absorption bands found above 200 cm^{-1} are likely to be due to iron oxide/hydroxide corrosion products that are typically formed at steel surfaces exposed to carbon dioxide media (Moiseeva & Rashevskaya, 2002; De Marco *et al.*, 2005). It is expected that only a thin layer of corrosion products would form in the presence of the MPY inhibitor, which shows high inhibiting efficiencies in carbon dioxide media (Pandarinathan *et al.*, 2013). The assignment of the absorption bands to the corrosion products is supported by the highest absorption intensities of these bands recorded at the high incidence angle (80°), which is typically observed for thin surface films, and by the changes in the intensities of the absorption bands with the decreasing incidence angle. The increase in absorption intensity with increasing incidence angle is due to the increased *p*-polarization vector of the incident radiation.

The spectral changes with the incidence angle in the region below 200 cm^{-1} are not definitively resolved at this point, including the unexpected maximum intensity of the band near 159 cm^{-1} at 55° and its opposite response with angle of incidence to the corrosion products (bands above 200 cm^{-1}) between 30° and 80°. The bands at 142 cm^{-1} and 159 cm^{-1} in the spectrum recorded at 30° are assigned to the ring distortions of the MPY molecule as they correspond to the bands at 146 cm^{-1} and 152 cm^{-1} in the spectrum from the pure MPY powder (Fig. 4); they suggest that MPY is present in its thiol ($C_4H_3N_2SH$) and thione ($C_4H_3N_2(H)S$) form, respectively. The absorption band near 142 cm^{-1} could also be related to the corrosion products formed at the steel surface. The assignments are tentative as a single band is not enough to indicate a specific compound or phase and the spectral changes can also be influenced by the change in sample area when the angle of incidence on the single-bounce reflectance accessory is changed.

At the MPY-free surface (Fig. 3), five absorption bands (143, 176, 190, 272 cm^{-1} and a broad band at 335 cm^{-1}) are identified from the spectrum recorded at the incidence angle of 30°. The absorption bands at 335 and 272 cm^{-1} can be tentatively assigned to a mixture of iron oxyhydroxides (FeOOH) and hematite (α-Fe_2O_3). The broadness of the absorption bands suggests amorphous states of these corrosion products being present. The positions of the absorption bands are not characteristic enough to distinguish between the different phases (α–δ) of the FeOOH. The absorption band at 335 cm^{-1} probably occurs due to contributions from both the feroxyhite (δ-FeOOH) and hematite (α-Fe_2O_3) (Nauer *et al.*, 1985; Carlson & Schwertmann, 1980; Labbé *et al.*, 2008; Serna *et al.*, 1987; Weckler & Lutz, 1998). The absorption band at 272 cm^{-1} is indicative of goethite (α-FeOOH), akaganeite (β-FeOOH) and lepidocrocite (γ-FeOOH) (Nauer *et al.*, 1985; Labbé *et al.*, 2008; Weckler & Lutz, 1998; Gehring & Hofmeister, 1994; Lewis & Farmer, 1986) with the phases α and γ likely to be formed at steels treated in carbon dioxide media (Moiseeva & Rashevskaya, 2002). The absorption bands at 176 and 190 cm^{-1} can be assigned to siderite ($FeCO_3$), as could the 335 cm^{-1} band, based on lattice vibrations of the carbonate ion in siderite (Angino, 1967; Blanchard *et al.*, 2009) and other calcite-structure minerals (White, 1974). The presence of siderite at this surface is supported by our mid-infrared analysis of the same steel sample, in which an absorption band near 1420 cm^{-1} was recorded and assigned to a vibrational mode (ν_3) of siderite (White, 1974). The broadening of absorption bands above 170 cm^{-1} may be related to the contribution from mixed metal ion carbonate structures (such as Mn-containing carbonates) (Brusentsova *et al.*, 2010). The absorption band near 143 cm^{-1} is not accounted for by the FeOOH, α-Fe_2O_3 or $FeCO_3$, but could again originate from the bulk corrosion products as at the MPY-treated surface.

4. Conclusions

The reflectance far-infrared spectra obtained from near smooth (R_q = 0.58 µm) and rough (R_q = 4.33 µm) corroded mild steel surfaces are influenced significantly with respect to their absorption intensities and spectral content by the incidence angle used (30, 55 and 80°). The following trends were determined:

(i) For low-roughness corroded surfaces (MPY-treated steel) the absorption intensity increases with increasing incidence angle for the majority of the absorption bands, but spectral content (absorption bands) also changes with changes in the incidence angle. This emphasizes the importance of using a range of incidence angles in the infrared analysis of low-roughness surfaces.

(ii) For high-roughness corroded surfaces (MPY-free steel) the absorption intensity increases with decreasing incidence angle due to the higher level of diffuse reflectance from corrosion products at lower angles of incidence (30°). This diffusion is reduced significantly at higher incidence angles. As the spectra are the results of diffuse and specular reflectance by corrosion products, the spectral content is not greatly affected by changes in the angle of incidence. Therefore, the use of low-incidence angles is favourable for the analysis of surfaces with high roughness.

This work is a first demonstration of the use of synchrotron FIR spectroscopy with variable incidence angles to analyse thin films and corrosion products at metal surfaces with respect to the surface roughness. It shows the benefit of varying the incidence angle and suggests that this strategy is applicable to all FIR spectroscopy studies on surfaces with uneven topography. Should the surface roughness be unknown prior to the FIR analysis, application of a wide range of incidence angles is recommended.

The infrared spectra absorption bands observed in this study are tentatively assigned to the MPY molecule, and corrosion products such as hematite, iron oxyhydroxides and iron carbonate.

This research was undertaken on the Far-infrared and high-resolution beamline at the Australian Synchrotron, Clayton, Australia. The assistance of Dr Dominique Appadoo and Ms Ruth Plathe is greatly acknowledged. The authors thank Dr Emilyn Chan for her help with the preliminary experimental work. The authors also thank Curtin University for a Curtin Research Fellowship (KL) and a Curtin International Postgraduate Research Scholarship (VP).

References

Angino, E. E. (1967). *Am. Mineral.* **52**, 137–148.
Aramaki, K., Ohi, M. & Uehara, J. (1992). *J. Electrochem. Soc.* **139**, 1525–1529.
Blanchard, M., Poitrasson, F., Méheut, M., Lazzeri, M., Mauri, F. & Balan, E. (2009). *Geochim. Cosmochim. Acta*, **73**, 6565–6578.
Brusentsova, T. N., Peale, R. E., Maukonen, D., Harlow, G. E., Boesenberg, J. S. & Ebel, D. (2010). *Am. Mineral.* **95**, 1515–1522.
Carlson, L. & Schwertmann, U. (1980). *Clays Clay Miner.* **28**, 272–280.
De Marco, R., Jiang, Z.-T., Pejcic, B. & Poinen, E. (2005). *J. Electrochem. Soc.* **152**, B389–B392.
Francis, S. A. & Ellison, A. H. (1959). *J. Opt. Soc. Am.* **49**, 131–138.
Gehring, A. U. & Hofmeister, A. M. (1994). *Clays Clay Miner.* **42**, 409–415.
Greenler, R. G. (1966). *J. Chem. Phys.* **44**, 310–315.
Hahn, F., Mathis, Y.-L., Bonnefont, A., Maillard, F. & Melendres, C. A. (2007). *J. Synchrotron Rad.* **14**, 446–448.
Hahn, F., Mathis, Y. L., Bonnefont, A., Maillard, F. & Melendres, C. A. (2008). *Infrared Phys. Technol.* **51**, 446–449.
Hahn, F. & Melendres, C. A. (2010). *J. Synchrotron Rad.* **17**, 81–85.
Labbé, J., Lédion, J. & Hui, F. (2008). *Corros. Sci.* **50**, 1228–1234.
Lewis, D. G. & Farmer, V. C. (1986). *Clay Miner.* **21**, 93–100.
Li Voti, R., Leahu, G. L., Gaetani, S., Sibilia, C., Violante, V., Castagna, E. & Bertolotti, M. (2009). *J. Opt. Soc. Am. B*, **26**, 1585–1593.
Melendres, C. A., Bowmaker, G. A., Leger, J. M. & Beden, B. (1998). *J. Electroanal. Chem.* **449**, 215–218.
Melendres, C. A. & Hahn, F. (1999). *J. Electroanal. Chem.* **463**, 258–261.
Melendres, C. A., Hahn, F. & Bowmaker, G. A. (2000). *Electrochim. Acta*, **46**, 9–13.
Moiseeva, L. S. & Rashevskaya, N. S. (2002). *Russ. J. Appl. Chem.* **75**, 1625–1633.

Nauer, G., Strecha, P., Brinda-Konopik, N. & Liptay, G. (1985). *J. Therm. Anal.* **30**, 813–830.
Nowak, M. J., Rostkowska, H. & Lapinski, L. (1991). *Spectrochim. Acta A*, **47**, 339–353.
Pandarinathan, V., Lepková, K., Bailey, S. I. & Gubner, R. (2013). *Corros. Sci.* **72**, 108–117.
Reznik, V. S., Akamsin, V. D., Khodyrev, Y. P., Galiakberov, R. M., Efremov, Y. Y. & Tiwari, L. (2008). *Corros. Sci.* **50**, 392–403.
Serna, C. J., Ocana, M. & Iglesias, J. E. (1987). *J. Phys. C*, **20**, 473–484.
Tripathi, G. N. R. & Clements, M. (2003). *J. Phys. Chem. B*, **107**, 11125–11132.
Weckler, B. & Lutz, H. D. (1998). *Eur. J. Solid State Inorg. Chem.* **35**, 531–544.
White, W. B. (1974). *The Infrared Spectra of Minerals*, edited by V. C. Farmer, pp. 227–284. Surrey: Adlard and Son.